Conformational Studies of Chiral Vinylogous Sulfonamidopeptides

Cesare Gennari,* Barbara Salom, Donatella Potenza,* Chiara Longari, Elena Fioravanzo, Oliviero Carugo, and Nicola Sardone

Abstract: The conformational preferences of chiral vinylogous aminosulfonic acids (vs-amino acids) and of the corresponding oligomers (vs-peptides) were investigated by a combination of X-ray crystallography, variable-temperature (VT) ^{1}H NMR spectroscopy, FT-IR spectroscopy, and NOE experiments. The major source of conformational freedom in the monomers is the rotation around the C–C bond connecting the double bond with the allylic stereocenter (N–C*–C=C). The allylic conformational preferences can be altered in the oligomers by the formation of secondary structures enforced by hydrogen bonding. Twelve-membered-ring hydrogen bonding is detected in the crystal structure of vs-dipeptide **9**, while fourteen-membered-ring hydrogen bonding is the most common folding pattern for the oligomers in chloroform solution. The experimental results are complemented by computer modeling: suitable force-field (FF) parameters for the unsaturated sulfonamide group were developed from ab initio calculations. A Goodman–Still systematic pseudo-Monte-Carlo search was used for the conformational search. The conformers were minimized in chloroform with the GB/SA model. The calculations correctly predicted both the size of the hydrogen-bonded ring and its relative importance, in agreement with the experimental data in solution.

Keywords
conformation · crystal structure · molecular modeling · NMR spectroscopy · sulfonamido-pseudopeptides

Introduction

Although during the past two decades a great deal of work has been devoted to the replacement of the scissile peptide bond with mimetic groups,[1, 2] relatively little is known about pseudopeptides characterized by the presence of the sulfonamido bond.[3a–h] This modification creates a peptide bond surrogate with significant changes in polarity, H-bonding ability and acid–base character (RSO_2–NHR′, $pK_a = 10–11$). Furthermore, the sulfonamido bond should show enhanced metabolic stability and structural similarity to the tetrahedral transition state involved in amide bond enzymatic hydrolysis.[3a–d] This makes sulfonamidopeptides interesting candidates for the development of protease inhibitors and new drugs.[3i–l] The oligomers and the polymers should also be interesting molecular scaffolds, with specific pseudopeptide backbone conformations based on the hydrogen-bonding network. Unfortunately α-aminosulfonamides are known to be unstable and to decompose immediately by fragmentation.[4] We have recently described the synthesis of chiral vinylogous aminosulfonic acids (vs-amino acids) starting from natural α-amino acids, the development of a straightforward protection–deprotection coupling chemistry for the sulfonamido bond, and the synthesis of sulfonamido-pseudopeptides by an iterative process, both in solution[5a, b] and in the solid phase.[5c] In collaboration with Clark Still at Columbia University and Peter Nestler at Cold Spring Harbor Laboratory, we have recently described the binding of tweezer-like molecular receptors based on vs-peptides to an encoded combinatorial tripeptide library, showing not only that vs-peptide-based receptors bind oligopeptides, but also that the binding selectivity is just as high as that of receptors built with α-amino acids.[5d]

In this paper we report on the conformational preferences of this new class of compounds. The goal is to study simple vs-amino acids and vs-dipeptides in great detail in order to devise a set of rules and trends useful for the interpretation of the more complex vs-tripeptides and vs-tetrapeptides. Intramolecular dipolar attraction, including hydrogen bonding, is expected to be a principal driving force for folding in these systems.

[*] Prof. Dr. C. Gennari, Dr. B. Salom, Dr. D. Potenza, C. Longari, E. Fioravanzo
Dipartimento di Chimica Organica e Industriale, Università di Milano
Centro CNR per lo Studio delle Sostanze Organiche Naturali
via G. Venezian 21, I-20133 Milan (Italy)
Fax: Int. code +(2)236-4369
e-mail: cesare@iumchx.chimorg.unimi.it
Dr. O. Carugo,[+] Dr. N. Sardone[+]
Dipartimento di Chimica Generale, Centro Grandi Strumenti
Università di Pavia, via Bassi 21, I-27100 Pavia (Italy)
Fax: Int. code +(382)42-2251
e-mail: nicola@elicona.unipv.it
[+] Questions on the X-ray structures should be addressed to these authors.

Results and Discussion

We have investigated the conformational preferences of the monomers **1**–**6** (Fig. 1) by a combination of X-ray crystallography (**1**–**3**), variable-temperature (VT) ^{1}H NMR spectroscopy,[6] and FT-IR spectroscopy.[6] Carbamate **7** and sulfonamide **8** were studied as reference compounds (Fig. 2). We have also studied the conformational preferences of the oligomers **9**–**13** (Fig. 3) by a combination of VT ^{1}H NMR spec-

0947-6539/96/0206-0644 $ 15.00+.25/0

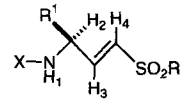

1	X = Boc	R^1 = Me	R= OMe
2	X = Boc	R^1 = *i*Pr	R= OEt
3	X = Boc	R^1 = Bn	R= OMe
4	X = Boc	R^1 = *t*Bu	R= OMe
5	X = Boc	R^1 = Me	R= $NH_{(5)}Bn$
6	X = SO_2Me	R^1 = Me	R= $NH_{(5)}Bn$

Fig. 1. Protected vinylogous aminosulfonic acids (vs-amino acids).

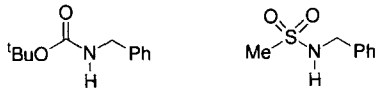

7 **8**

Fig. 2. Reference compounds.

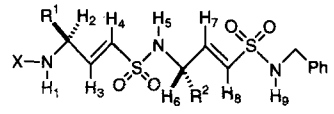

9 X = Boc R^1 = Me R^2= *i*Pr
10 X = SO_2Me R^1 = Me R^2= *i*Pr

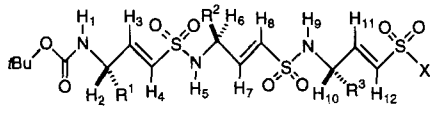

11 X = OEt R^1 = CH_2Ph R^2 = Me R^3= *i*Pr
12 X = $NH_{(13)}Bn$ R^1 = CH_2Ph R^2 = Me R^3= *i*Pr

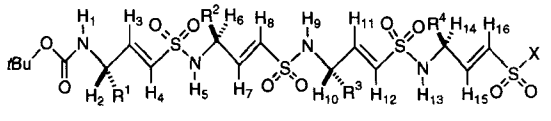

13 X = $NH_{(17)}Bn$ R^1 = CH_2*i*Pr R^2 = CH_2Ph R^3 = Me R^4= *i*Pr

Fig. 3. Protected vinylogous sulfonamidopeptides (vs-peptides).

troscopy, FT-IR spectroscopy, and nuclear Overhauser effect (NOE) experiments. Vs-dipeptide **9** was also investigated in the solid state by X-ray crystallography. The conformational preferences of the oligomers **9**–**13** were studied in an organic solvent (chloroform) in an effort to elucidate the manner in which noncovalent interactions control the adoption of molecular conformations.

X-ray crystallography: X-ray crystallographic analysis provided the first insight into the conformational preferences of this new family of compounds and gave detailed parameters for their molecular geometry. The crystal structures of the monomers L-Boc–vs-Ala–OMe (**1**), L-Boc–vs-Val–OEt (**2**), and L-Boc–vs-Phe–OMe (**3**) are shown in Figures 4–6 (Boc = *tert*-butyloxycarbonyl).[7]

The conformational preference of the allylic stereocenter with respect to the double bond does not appear well-defined: inspection of the crystal structures reveals that either the CH-eclipsed conformer [as in **1**, H–C6–C8=C9 = 0.9(5)°], the CN-eclipsed conformer [as in **3**, N–C6–C8=C9 = −10.9(4)°], or a more staggered conformer [as in **2**, H–C6–C8=C9 = 47.6(8)°] are all possible. The allylic conformational

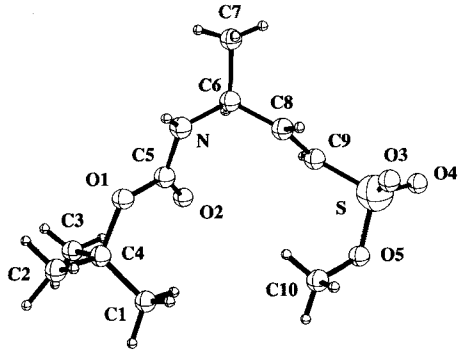

1

Fig. 4. X-ray crystal structure of L-Boc–vs-Ala–OMe (**1**). H–C6–C8=C9 = 0.9(5)°; N–C6–C8=C9 = 112.9(5)°.

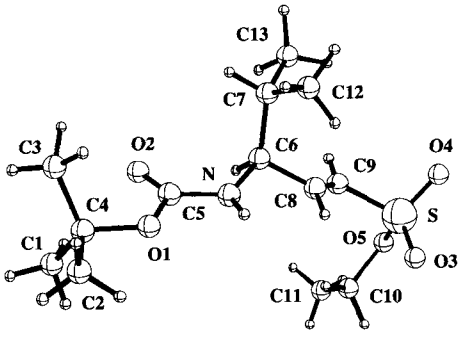

2

Fig. 5. X-ray crystal structure of L-Boc–vs-Val–OEt (**2**). H–C6–C8=C9 = 47.6(8)°; N–C6–C8=C9 = 151.1(8)°.

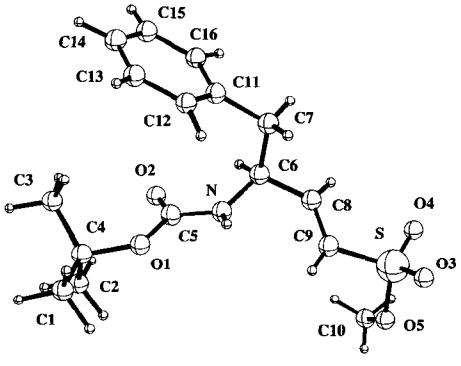

3

Fig. 6. X-ray crystal structure of L-Boc–vs-Phe–OMe **3**. H–C6–C8=C9 = −126.3(4)°; N–C6–C8=C9 = −10.9(4)°.

preferences can be altered in the oligomers by the formation of organized secondary structures enforced by hydrogen bonding. For example, in the crystal structure the vs-dipeptide L-Boc–vs-Ala–L-vs-Val–NHBn (**9**, Fig. 7) shows an intramolecular hydrogen bond between the hydrogen of the Boc–NH group and the oxygen of the SO_2NHBn group forming a twelve-membered ring [(N1)H–O6 = 2.22(5) Å; N1–H(N1)–O6 = 155(5)°; N1–O6 = 3.037(5) Å]. The folded twelve-membered structure is further stabilized by a CH–π-arene interaction[8] between the Boc *tert*-butyl group and the NHBn aromatic ring [H–ring plane distance = 2.948(7) Å]. The strongest hydrogen bond in this crystal structure is intermolecular, between the oxygen of

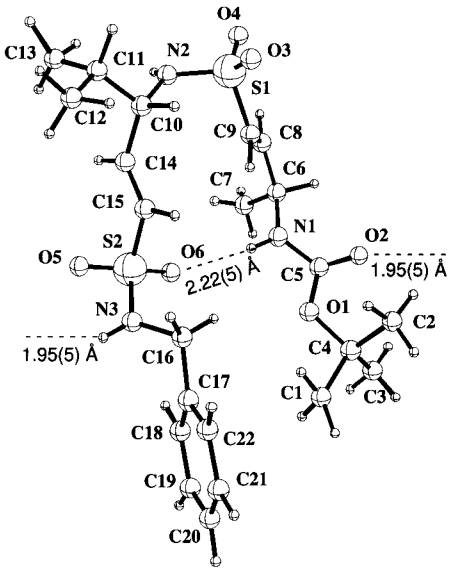

9

Fig. 7. X-ray crystal structure of L-Boc-vs-Ala-L-vs-Val-NHBn (**9**). H-C10-C14=C15 = -2.5(7)°; N2-C10-C14=C15 = 111.4(5)°; H-C6-C8=C9 = -119.5(7)°; N1-C6-C8=C9 = 0.7(7)°.

the Boc group and the hydrogen of the SO_2NHBn group of a neighbor vs-dipeptide [(N3)H^{ii}-O2^{i} = 1.95(5) Å; N3^{ii}-H(N3)^{ii}-O2^{i} = 170(5)°; N3^{ii}-O2^{i} = 2.804(4) Å, symmetry codes: $^{i} = x, y, z$; $^{ii} = x-1, y+1, z$].

In the structure in chloroform solution, this hydrogen bond is intramolecular and gives rise to a tightly hydrogen-bonded fourteen-membered ring (see the discussion of conformational preferences in solution). Inspection of the crystal structure of the vs-dipeptide L-Boc-vs-Ala-L-vs-Val-NHBn (**9**, Fig. 7) reveals the presence of two different allylic conformers, one CH-eclipsed [in the vs-Val subunit, H-C10-C14=C15 = -2.5(7)°, N2-C10-C14=C15 = 111.4(5)°] and one CN-eclipsed [in the vs-Ala subunit, N1-C6-C8=C9 = 0.7(7)°, H-C6-C8=C9 = -119.5(7)°]. It is interesting to observe that vs-Ala is CH-eclipsed in the monomer (**1**, Fig. 4), and CN-eclipsed in the vs-dipeptide (**9**, Fig. 7), while vs-Val is partially staggered in the monomer (**2**, Fig. 5) and CH-eclipsed in the vs-dipeptide (**9**, Fig. 7). This is again indicative of a rather flat potential energy surface including two eclipsed conformers (CN and CH) of similar energy.

The conformational preferences around the sulfonate ester or the sulfonamide bond are quite similar in all the crystal structures examined, and show a gauche arrangement (C-S-O-C = 69-78°; C-S-N-C = 62-69°) of the two carbon chains. The double bond is nearly eclipsed by one of the two S=O bonds in the α,β-unsaturated sulfonate esters (C=C-S=O = 4-14°) and in the sulfonamides (C=C-S=O = 11-31°). In the sulfonamides, the hydrogen of the allylic stereocenter tends to eclipse the sulfur atom (S-N-C-H = 23°) (Fig. 8).

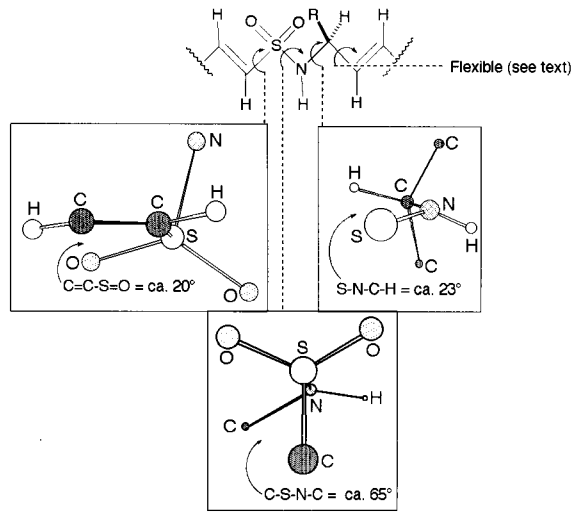

Fig. 8. Average C-N-S-C dihedral angles from X-ray crystal structure analysis.

VT ^{1}H NMR spectroscopy of the monomers and of the oligomers—conformational studies based on ^3J couplings: We have used VT ^{1}H NMR spectroscopy to study the conformational preferences in solution (chloroform). Our choice of chloroform was motivated by interest in the conformational preferences of the sulfonamido-pseudopeptides in a solvent of low dielectric constant and polarity.[9]

Initially we studied the conformational preferences of the allylic stereocenters. The rotation around the allylic C*(sp^3)-C(sp^2) bond was monitored in chloroform solution by the ^{1}H NMR coupling (^3J) between the protons H2 (at the stereocenter) and H3 (at the double bond) at variable temperature for the compounds in Figure 1. In the temperature range of 240-300 K, all peaks of the NMR spectra remained sharp, indicating rapid rotation around all single C-C bonds; the coupling constants measured are therefore weighted averages of all rotamers. The *trans* three-bond coupling ($J \approx 10$ Hz) is about five times as large as the *gauche* coupling ($J \approx 2$ Hz). Therefore, a change in the population of the CH2-eclipsed rotamer will in turn cause a change in the observed coupling constant (^3J). To facilitate analysis of the data, we have introduced $\Delta J/\Delta T$ values (Table 1),

Table 1. $\Delta J/\Delta T$ (10^3 Hz K^{-1}) of compounds **1**-**6** and **9**-**13** for 1 mM $CDCl_3$ solutions in the 240-300 K temperature range.

$\Delta J/\Delta T$	1	2	3	4	5	6	9	10	11	12	13 [a]
H2-H3	0.0	0.0	0.0	6.1	14.0	14.0	-8.1	28.0	0.0	-19.6	- [b]
H6-H7							16.3	7.1	9.1	4.8	19.6
H10-H11									-6.1	5.0	68.4
H14-H15											19.6

[a] Measured in the 250-300 K temperature range. [b] Not detectable.

which are calculated by dividing the coupling constant change over the temperature range at which the change in coupling was observed. Physically, a positive $\Delta J/\Delta T$ value indicates that the CN-eclipsed form is more stable at lower temperatures, while a negative $\Delta J/\Delta T$ value indicates that the CH-eclipsed rotamer is more stable.[10]

The observed coupling constants for compounds **1**-**3** (typical value 4.88 Hz) remain essentially unchanged at different temperatures. In contrast, $\Delta J/\Delta T$ values for compounds **4**-**6** are positive; this indicates a preference for the CN-eclipsed conformer. It is interesting to observe that oligomers **9**, **11**, and **12** show a preference for the CH-eclipsed rotamer (negative $\Delta J/\Delta T$ value) for one of the allylic stereocenters (Table 1). As this trend is not observed in the monomers, it is probable that the allylic conformational preferences are altered in the oligomers by the formation of secondary structures enforced by hydrogen bonding (see the discussion below).

^3J coupling constants between the sulfonamide NH and the hydrogen of the allylic stereocenter are quite large (9-10 Hz) for all compounds examined (**9**-**12**) and tend to increase at lower

0947-6539/96/0206-0646 $ 15.00+.25/0 Chem. Eur. J. 1996, 2, No. 6

temperatures. This behavior is indicative of quite a large dihedral angle H–N–C*–H, in agreement with the X-ray analysis (see Fig. 8).

VT ^{1}H NMR spectroscopy of the monomers and of the oligomers—detection of intramolecular hydrogen bonding: Vinylogous sulfonamidopeptides (**9**–**13**) show two aspects of the covalent structure that are essential for the formation of intramolecular hydrogen bonds: a) the repeating backbone structure should contain both hydrogen-bond donors (NH) and hydrogen-bond acceptors (C=O and S=O); b) the covalent spacing of these repeating hydrogen-bonding groups should be such that interactions between nearest neighbor sulfonamide groups are not favorable.

In order to gain insight into the conformational behavior of monomers **1**–**6** and oligomers **9**–**13**, we have analysed the NH chemical shifts of these compounds. An amide NH chemical shift is very sensitive to that proton's hydrogen-bonding status. Typically, it moves upfield as the temperature is raised, which is interpreted as indicating a heat-induced disruption of hydrogen bonding. Equilibration between hydrogen-bonded and non-hydrogen-bonded states is usually fast on the NMR timescale, which means that observed chemical shifts are weighted averages of the observed chemical shifts of the contributing states.[6]

The resonances of NH protons of all compounds described below are resolved at all temperatures studied. These resonances were assigned either by their splitting patterns or by homonuclear decoupling experiments.

For all compounds described in the following text, NMR experiments show that the NH proton chemical shifts are independent of concentration at 300 K, at or below 5×10^{-3} M, and therefore all experiments were conducted in 1×10^{-3} M solutions. Variable-concentration ^{1}H NMR data indicate that the NH protons can be additionally classified in two different categories: protons whose chemical shifts are independent of concentration at 240 K in the range 5×10^{-3}–1×10^{-3} M (all NH protons of compounds **1**–**5**, **7**–**9**, **11**, and **13**), and protons whose chemical shifts are dependent on concentration at 240 K in the same concentration range (selected NH protons of compounds **6**, **10**, and **12**). Figure 9 shows the effect of concentration on the NH chemical shifts for compounds **6** and **10** over the range 1–5×10^{-3} M at 240 K. These data indicate that monomer **6** aggregates avidly in this concentration range (both H1 and H5 chemical shifts change greatly). In the case of vs-dipeptide **10**, the chemical shifts of H1 and H9 are concentration-independent, while that of H5 is not; a possible explanation for this behavior is the involvement of H1 and H9 in intramolecular ring formation driven by hydrogen bonding (see the discussion below for vs-peptides **10** and **12**) that leaves H5 available for a selective intermolecular association. VT ^{1}H NMR experiments (300–240 K; 1×10^{-3} M chloroform solution) conducted with the aim of detecting intramolecular hydrogen bonding are reliable only for the first category of protons, while for the second

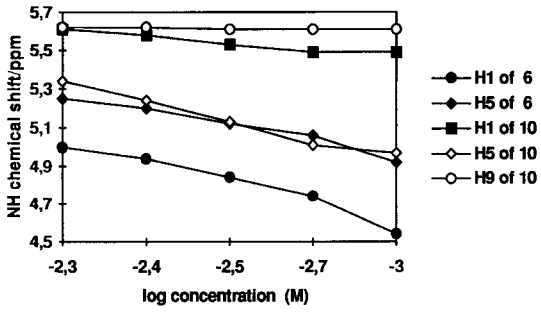

Fig. 9. NH ^{1}H NMR chemical shifts of compounds **6** and **10** in $CDCl_3$ at 240 K as a function of concentration.

category they are confused and invalidated by the formation of intermolecular aggregates.[11]

For relatively simple (sulfono)amides, including small vs-peptides, variable-temperature ^{1}H NMR data obtained in a weakly polar solvent like chloroform (specifically the temperature dependences of (sulfono)amide proton chemical shifts, $\Delta\delta$(NH)/ΔT) can provide qualitative and sometimes quantitative information on the thermodynamic relationships among alternative folding patterns, when appropriate reference molecules are available.[6] In a flexible molecule, small $\Delta\delta$(NH)/ΔT values have been associated with amide protons that are either completely locked in an intramolecular hydrogen bond or completely free of hydrogen bonding over the temperature range examined. These two extreme possibilities can be distinguished either by analysis of the IR spectrum or by observation of the chemical shift value in comparison with the appropriate reference molecules. Table 2 shows the $\Delta\delta$(NH)/ΔT values derived from the VT NMR data for compounds **1**–**5** and **7**–**13**.

The $\Delta\delta$(NH)/ΔT signature for the amide proton of **7** represents the behavior of a carbamate proton in the non-hydrogen-bonded state. This resonance appears in the range $\delta = 4.82$–4.88, and the temperature dependence is small (-1.0×10^{-3} ppm K^{-1}) (Table 2). The $\Delta\delta$(NH)/ΔT for sulfonamide **8** is also relatively small (-2.8×10^{-3} ppm K^{-1}, Table 2); the NH chemical shift of **8** represents the behavior of a typical sulfonamide in the non-hydrogen-bonded state.

The presence of a *trans* double bond in vs-amino acids and vs-peptides prevents seven-membered-ring hydrogen bonding between S=O and HN. As expected, compounds **1**–**4** show very small $\Delta\delta$(NH)/ΔT values. Monomer **5** could experience nine-membered-ring intramolecular hydrogen bonding with the Boc carbonyl group (H5–O=C). Comparison of the H1 and H5 NMR data of **5** with the data for **7** and **8** indicates that the NH protons of **5** are *not* involved in hydrogen bonding: firstly, the $\Delta\delta$(NH)/ΔT signatures for H1 and H5 of **5** are small (Table 2); secondly, the H1 and H5 resonances ($\delta = 4.38$ and 4.40, respectively, at 300 K; 4.56 and 4.49, respectively, at 240 K) are slightly upfield of the NH resonances of the reference

Table 2. $\Delta\delta$(NH)/ΔT (10^{-3} ppm K^{-1}) of compounds **1**–**5** and **7**–**13** for 1 mM $CDCl_3$ solutions in the 240–300 K temperature range.

$\Delta\delta/\Delta T$	1	2	3	4	5	7	8	9	10	11	12	13 [b]
NH1	−1.6	−1.3	−1	−1.4	−2.4	−1.0	−2.8	−0.6	−10.2	−0.7	−0.4	7
NH5					−2.1			−3.3	-[a]	−1.8	-[a]	2
NH9								−11.1	−6.4	−7.4	−8.1	−9
NH13											−5.1	−6.2
NH17												−7

[a] The $\Delta\delta$(NH)/ΔT values are reported only for protons whose shifts are concentration-independent in the temperature range examined. [b] Measured in the 250–300 K temperature range.

  0947-6539/96/0206-0647 $ 15.00+.25/0

compounds **8** ($\delta = 4.50$ at 300 K and 4.69 at 240 K) and **7** ($\delta = 4.82$ at 300 K and 4.91 at 240 K) throughout the temperature range examined (240–300 K). This inability to form intramolecular hydrogen bonds between the nearest neighbor amide-type groups leading to small (9-membered) rings has a major consequence for the hydrogen bonding of the oligomers (see below).[6e]

A sulfonamide NH is more acidic ($pK_a \approx 10-11$) and therefore is a stronger hydrogen-bond donor than a carbamate NH. Clear evidence of this behavior is obtained by adding increasing amounts of [D$_6$]DMSO to a 1×10^{-3} M solution of **5** in $CDCl_3$ at room temperature. The sulfonamide NH (H5) moves to lower field more rapidly than the carbamate NH (H1): on addition of 3000 equiv of DMSO H5 moves from $\delta = 4.42$ to a plateau value of 6.90, while H1 moves from 4.43 to 5.48.

All three NH proton (H1, H5, H9) chemical shifts of vs-dipeptide **9** were shown to be concentration-independent between 1 and 5×10^{-3} M at both 300 K and 240 K, which is consistent with a monomeric state throught this range. Vs-dipeptide **9** shows a strong preference for a single fourteen-membered-ring hydrogen-bonded species (H9–O=C). This is quite evident from the chemical shifts of H9, which are consistently downfield (1.2–2.0 ppm) of the H5 proton and the NH proton of the reference compound **8** in the 240–300 K temperature range. Moreover, the $\Delta\delta(NH)/\Delta T$ value of H9 is quite large (-11.1×10^{-3} ppm K^{-1}, Table 2), compared with H5 and H1 of the same compound (-3.3×10^{-3} ppm K^{-1} and -0.6×10^{-3} ppm K^{-1}, respectively, Table 2). Figure 10 shows the temperature dependence of the amide proton NMR chemical shifts for 1 mM samples of vs-dipeptides **9** and **10**.

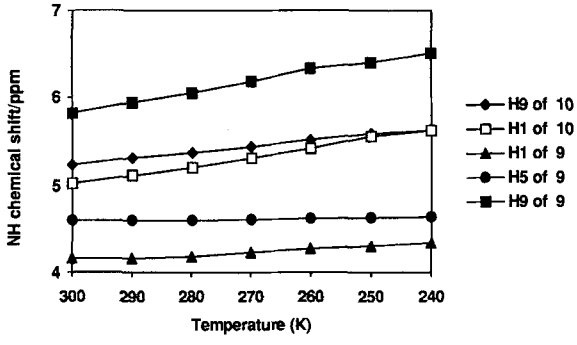

Fig. 10. NH ^{1}H NMR chemical shifts of vs-dipeptides **9** and **10** in 1 mM $CDCl_3$ solutions as a function of temperature.

Vs-dipeptide **9** could in principle also form a twelve-membered-ring hydrogen-bonded species (H1–O=S). However, both the chemical shift and the $\Delta\delta(NH)/\Delta T$ value of H1 exclude this possibility. The formation of a tight fourteen-membered-ring hydrogen bond (H9–O=C) is also plainly demonstrated at room temperature by the strong NOE at H9 upon irradiation of the *t*Bu of the Boc group and the IR shift to lower frequencies of ν(C=O) (which appears at 1705 cm^{-1}) and ν(N–H) (3253 cm^{-1}), both the bonds involved in the hydrogen bonding (see the IR section below). These observations indicate that **9** adopts a compact intramolecularly hydrogen-bonded folding pattern that is sufficiently robust to inhibit intermolecular association.

The allylic conformational preferences of vs-dipeptide **9** are also strongly altered by the formation of the fourteen-membered-ring hydrogen-bonded species. The $\Delta J/\Delta T$ value for the vs-Val subunit is strongly positive (16.3×10^{-3} Hz K^{-1}, Table 1), indicating a preference for the CN-eclipsed rotamer, while for the vs-Ala subunit it is negative (-8.1×10^{-3} Hz K^{-1}, Table 1), indicating a preference for the CH-eclipsed rotamer (compare with the $\Delta J/\Delta T$ values of the monomers **1** and **2**, Table 1).

In vs-dipeptide **10** the H1 and H9 chemical shifts are independent of concentration at 240 K, while the H5 chemical shift is not, even below 1×10^{-3} M (Fig. 9), and therefore its $\Delta\delta(NH)/\Delta T$ value is not significant. The other two sulfonamide hydrogens (H1, H9) show relatively large $\Delta\delta(NH)/\Delta T$ values (Table 2, Figure 10). In particular, H1 can form a hydrogen-bonded twelve-membered ring (H1–O=S), and H9 a hydrogen-bonded fourteen-membered ring (H9–O=C). Competition between the two different folding patterns probably contributes to the diminution of the population of each hydrogen-bonded ring (compare, for example, vs-dipeptide **9** where only one hydrogen-bonding pattern is present, Fig. 10). The sulfonamide proton H1 chemical shift shows a larger temperature dependence than that of H9, which indicates that formation of the twelve-membered hydrogen-bonded ring is enthalpically more favored than that of the fourteen-membered ring.

As with vs-dipeptide **9**, the allylic conformational preferences are also strongly altered in **10** by the formation of the hydrogen-bonded species. The $\Delta J/\Delta T$ values for both the vs-Ala and vs-Val subunits of vs-dipeptide **10** are positive (28.0×10^{-3} and 7.1×10^{-3} Hz K^{-1}, respectively, Table 1) indicating a distinct preference for the CN-eclipsed rotamers (compare with the $\Delta J/\Delta T$ values of the monomers **1** and **2**, Table 1).

Vs-tripeptide **11** has the same type and number of NH protons as **9**. The presence of an additional vinylogous sulfonoester unit in **11** does not alter its conformational preferences compared with **9**. Vs-tripeptide **11** also shows a strong preference for a single fourteen-membered-ring hydrogen-bonded species (H9–O=C). The resonance of H9 appears at $\delta = 5.8-6.2$ in the 240–300 K temperature range. Moreover, the $\Delta\delta(NH)/\Delta T$ value of H9 is rather large (-7.4×10^{-3} ppm K^{-1}, Table 2), compared with H5 and H1 (-1.8×10^{-3} ppm K^{-1} and -0.7×10^{-3} ppm K^{-1}, Table 2). Figure 11 shows the temperature dependence of the amide proton NMR chemical shifts for 1 mM samples of vs-tripeptides **11** and **12**.

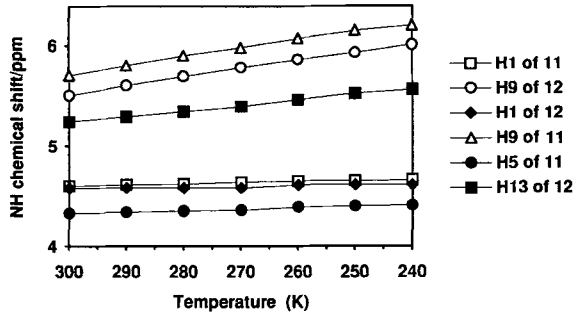

Fig. 11. NH ^{1}H NMR chemical shifts of vs-tripeptides **11** and **12** in 1 mM $CDCl_3$ solutions as a function of temperature.

Formation of the fourteen-membered-ring hydrogen-bonded species alters the allylic conformational preferences of vs-tripeptide **11**. The $\Delta J/\Delta T$ value for the vs-Val subunit of vs-tripeptide **11** is negative (-6.1×10^{-3} Hz K^{-1}, Table 1), indicating a preference for the CH-eclipsed rotamer, while it is positive for the vs-Ala subunit (9.1×10^{-3} Hz K^{-1}, Table 1) indicating a preference for the CN-eclipsed rotamer (compare with the $\Delta J/\Delta T$ values of vs-dipeptide **9** and of the monomers **1** and **2**, Table 1).

0947-6539/96/0206-0648 $ 15.00+.25/0 Chem. Eur. J. 1996, 2, No. 6

In vs-tripeptide **12**, H1, H9 and H13 chemical shifts are independent of concentration at 240 K, while H5 chemical shift is not, even below 1×10^{-3} M, and therefore its $\Delta\delta(NH)/\Delta T$ value is not significant (see Fig. 11). Vs-tripeptide **12** has one more NH group, and therefore it experiences more competition between the various possible hydrogen-bonded rings. H13 can form either a fourteen-membered hydrogen-bonded ring with the O=S group of the vs-Phe subunit, or a nineteen-membered ring with the carbamate C=O group; H9 can form a fourteen-membered ring with the carbamate C=O group. Comparison of the NMR data of H9 and H13 shows that δ H9 is always farther downfield from δ H13, indicating that the fourteen-membered ring of H9 and C=O occurs more frequently than the rings involving H13. The formation of these hydrogen-bonded rings is evident from the downfield shift of H9 and H13 and their $\Delta\delta(NH)/\Delta T$ values (Fig. 11, Table 2).

The chemical shift value for H9 of vs-tripeptide **11** is constantly downfield of H9 of vs-tripeptide **12** at all temperatures (Fig. 11). These differences should largely reflect differences in the extent of the internal hydrogen bonding of these protons. Competition between the alternative folding patterns (H9–O=C vs. H13–O=C) probably diminishes the population of the hydrogen-bonded species involving H9 of **12**.

Strong Overhauser effects were observed for vs-tripeptide **12** at room temperature between H11 and H1 or H2 (isochronous), H9 and *t*Bu, H6 and H1 or H2 (isochronous), *t*Bu and CH_2 of the SO_2NHCH_2Ph group, and are indicative of a distinct folding of the molecule. The IR data are treated below.

The ^{1}H NMR spectrum of vs-tetrapeptide **13** is fairly complicated because of extensive signal overlap; the resonances of all protons were assigned at various temperatures in the 250–300 K range by homonuclear correlation spectroscopy (COSY and TOCSY). Variable-temperature NMR data for H1 and H5 show positive $\Delta\delta(NH)/\Delta T$ values, in complete contrast to all other cases (Table 2). The strong negative $\Delta\delta(NH)/\Delta T$ value for H9 is indicative either of the usual fourteen-membered-ring hydrogen bonding with the carbamate C=O (see the discussion of IR data below) or of hydrogen bonding with the available S=O groups. H13 and H17 show rather large negative $\Delta\delta(NH)/\Delta T$ values, which indicates their involvement in various hydrogen-bonded rings. These rings involving H9, H13, and H17 are probably enthalpically favored compared with other rings involving H1 and H5, and are therefore more common at lower temperatures.

Discussion of IR data: Hydrogen-bonding equilibria are slow on the IR timescale, in contrast to the NMR timescale, giving rise to discrete N–H stretch bands for hydrogen-bonded and non-hydrogen-bonded states of a given secondary amide group. IR has the disadvantage, relative to NMR, of signal overlap when more than one N–H group is present.[6] Table 3 shows the N–H stretch region FT-IR spectral data for 1 mM $CHCl_3$ solutions of sulfonamides **5**–**13** in $CHCl_3$ at room temperature. No intermolecular amide–amide hydrogen bonding is detectable in a solution of **7** and **8**. The only absorption observed in the N–H stretch region [ν(N–H)] under these conditions occurs at 3458.5 cm^{-1} for **7** and at 3394.1 cm^{-1} for **8**. We shall refer to these N–H stretch absorptions as indicative of a non-hydrogen-bonded state to distinguish them from IR absorptions arising from a hydrogen-bonded state.

Monomers **5** and **6** experience no intramolecular hydrogen bonding at room temperature (Table 3).

Vs-dipeptide **9** displays three signals in the N–H stretch region in 1 mM $CHCl_3$ solution: a broad signal at 3252 cm^{-1} corresponding to an intramolecularly hydrogen-bonded sulfonamide hydrogen, a sharp signal at 3390 cm^{-1} corresponding to a non-hydrogen-bonded sulfonamide hydrogen, and a sharp signal at 3446 cm^{-1} corresponding to a non-hydrogen-bonded carbamate hydrogen. Vs-dipeptide **10** equilibrates between non-hydrogen-bonded and intramolecularly hydrogen-bonded states as shown by the presence of non-hydrogen-bonded (3394 cm^{-1}, sharp) and hydrogen-bonded (3281 cm^{-1}, broad) signals in the N–H stretch region. Vs-tripeptides **11** and **12** display three signals in the N–H stretch region in 1 mM $CHCl_3$ solution: a broad signal (3389 and 3390 cm^{-1}, respectively) corresponding to a non-hydrogen-bonded sulfonamide hydrogen, a sharp signal (3249 and 3252 cm^{-1}, respectively) corresponding to an intramolecularly hydrogen-bonded sulfonamide hydrogen, and a sharp signal (3444 and 3450 cm^{-1}, respectively) corresponding to a non-hydrogen-bonded carbamate hydrogen. The bands at 3450, 3386, 3265 cm^{-1} for vs-tetrapeptide **13** result from non-hydrogen-bonded carbamate hydrogen, non-hydrogen-bonded sulfonamide hydrogen, and H-bonded sulfonamide hydrogen, respectively.

Table 3. IR spectra of compounds **5**–**13** for 1 mM $CHCl_3$ solutions at 300 K.

Compounds	ν(NH) non bonded (carbamate)	ν(NH) non bonded (sulfonamide)	ν(NH) bonded (sulfonamide)	ν(C=O)
5	3458	3386		1713
6		3386		
7	3458			1730
8		3394		
9	3446	3390	3252	1705
10		3394	3281	
11	3450	3390	3252	1699, 1717 [a]
12	3444	3389	3249	1698, 1719 [a]
13	3450	3386	3265	1696, 1713

[a] Shoulder.

In the C=O stretch region (Table 3), carbamate **7** shows a strong band at 1730 cm^{-1}, while vs-dipeptide **9** has a single band at 1705 cm^{-1}, that is, the band shifts approximately 25 cm^{-1} to lower frequency owing to hydrogen bonding. Unlike the variable-temperature NMR data (Table 2, Fig. 10), which show the presence of an equilibrium between hydrogen-bonded and non-hydrogen-bonded states, IR data do not detect these two different species, probably because the H-bonded induced shift is similar to the width of the band. However, vs-tripeptides **11** and **12** show two bands, a strong band (1698 and 1699 cm^{-1}, respectively) corresponding to a hydrogen-bonded carbonyl group, and a shoulder (1719 and 1717 cm^{-1}, respectively) corresponding to a non-hydrogen-bonded carbonyl group. Vs-tetrapeptide **13** shows two separate bands of about the same intensity, at 1696 and 1713 cm^{-1}, corresponding to a hydrogen-bonded and a non-hydrogen-bonded carbonyl group, respectively.

Thermodynamic analysis of the folding of the oligomers: For an amide proton equilibrating between a non-hydrogen-bonded state and a hydrogen-bonded state, the equilibrium constant for the two-state system may be calculated from δ(NH) if the limiting chemical shifts for the non-hydrogen-bonded and hydrogen-bonded states are known at any temperature [Eq. (1), where δ_{obs}

$$K_{eq} = (\delta_{obs} - \delta_n)/(\delta_b - \delta_{obs}) \quad (1)$$

is the observed chemical shift, δ_n is the limiting chemical shift for the non-hydrogen-bonded state, and δ_b is the limiting chemical shift for the fully hydrogen-bonded state]. In $CDCl_3$ the chem-

ical shift of the sulfonamide NH (H 5) of **5** can serve as δ_n at all temperatures. Determining the limiting chemical shift for the intramolecularly hydrogen-bonded state is more problematic, because both the absolute value and the temperature dependence of δ_b may vary with hydrogen-bond geometry. We estimated the required value of δ_b at room temperature from the chemical shift of the sulfonamide NH of **5** in 1 mM $CDCl_3$ solution after the addition of 3000 equiv of DMSO. We also assumed that this value applies to a hydrogen bond of optimum geometry.

Table 4 shows the results of van't Hoff analyses of the conformational equilibria of vs-peptides **9**–**12** based on Equation (1).

Table 4. Summary of thermodynamic parameters for vs-peptides **9**–**12**.

	9 (H9)	**10** (H1)	**10** (H9)	**11** (H9)	**12** (H9)	**12** (H13)
ΔH^0 (kcal mol^{-1})	−3.4	−2.3	−1.3	−1.9	−1.7	−1.2
ΔS^0 (eu)	−10.7	−8.3	−5.6	−5.6	−6.2	−5.3
correlation coeff.	0.998	0.994	0.986	0.991	0.992	0.992

The data shown in Table 4 imply that the intramolecularly hydrogen-bonded states are more enthalpically favorable than the non-hydrogen-bonded states, but are less favorable entropically. Obviously, the hydrogen-bonded and the nonbonded state are not single conformations, but refer to all possible conformers.

Computer modeling: Although the sulfonamide group is not specifically parametrized in the most popular force fields, ab initio studies of the sulfonamide group have been reported,[12] and the corresponding FF parameters have been developed by the appropriate combination of ab initio data with specific geometric features extracted from crystal structures.[12a,d] We undertook an ab initio study of the α,β-unsaturated sulfonamide CH_2=CH–SO_2–NHMe (**14**) in order to develop the torsional parameters for the C(sp^2)–C(sp^2)–S–N dihedral angle. Bond lengths and bond angles were calculated by averaging the values from the ab initio data. The newly developed parameters were added to the previously reported MM2 force-field parameters for the sulfonamide group[12a,d] (the complete force-field substructure is reported in Table 5). Bond dipole moments were assigned to stretching interactions in the sulfonamide substructure (Table 5) so that partial atomic charges were equal to half of the RHF/6-31G* Mulliken charges.[12a,d] Ab initio molecular orbital calculations were carried out with the Gaussian 90 programs:[13] the ab initio calculated (RHF/6-31G*) conformers for **14** (**14a**–**e**) are shown in Figure 12 with the respective relative energies. The conformational minima were located with 30° resolution around the C=C–S–N torsion angle, starting from the two different conformations for the C–S–N–C dihedral angle (99 and 72°).[12a] The force-field torsional parameters for the C(sp^2)=C(sp^2)–S–N dihedral angle (V_1 = 1.8, V_2 = −1.6, V_3 = −1.4) were developed by trial and error, in order to reproduce geometries and relative energies of the ab initio calculated structures. The differences between the ab initio and the force-field calculated relative energies, and between the ab initio and the force-field calculated C=C–S–N dihedral angles, are reported in Table 6.

Molecular modeling studies were carried out to gain insight into preferred conformations for intramolecularly hydrogen-bonded forms of the sulfonamido oligomers and relative stabilities of the conformers that make up the various hydrogen-bonded families.[6d,14] The ratios between the various families of hydrogen-bonded and non-hydrogen-bonded conformations were calculated by a Boltzmann distribution at 298 K of the family conformers within 2.0 kcal mol^{-1} above the global minimum. These studies were not intended to evaluate quantitatively the relative energetics of intramolecularly hydrogen-bonded and non-hydrogen-bonded conformations, but rather to

Table 5. MM2 Force-field substructure (MacroModel format) for the vinylogous sulfonamidopeptides. The first character of a line in the MacroModel force-field substructure describes the contents of that line: C indicates a comment, 1 specifies constants for stretching interactions, 2 specifies constants for bending interactions, 3 specifies constants for stretch-bend interactions, 4 specifies constants for dihedral interactions, and 9 specifies substructure linear notation; numbers < 0 indicate the format for subsequent statements (e.g., −2 indicates special substructure interactions).

C	Sulfonamide						
9	O2=S1–N3 [a]						
−2							
					[b]	[c]	[d]
1	3	H3			1.0020	8.0300	−0.9600
1	2	3			1.6500	5.8300	0.7900
1	1	2			1.4350	11.6400	−2.4000
1	3	C3			1.4400	5.4600	−0.9700
1	2	C3			1.7870	4.0900	−0.9000
1	3	Lp			0.6000	6.1000	
1	2	C2			1.7600	4.0900	−0.9000
					[e]	[f]	
2	C3	3	Lp		100.0000	0.5000	
2	H3	3	Lp		100.0000	0.5000	
2	Lp	3	2		100.0000	0.5000	
2	H3	3	2		114.7200	0.7522	
2	1	2	O2		122.0800	1.5081	
2	1	2	3		109.0600	1.3971	
2	C3	3	H3		115.6100	0.9711	
2	C3	3	2		111.1900	0.6890	
2	C3	2	3		104.0700	1.4405	
2	C3	2	1		107.6200	1.1688	
2	C2	2	1		107.7000	1.1688	
2	C2	2	3		104.3000	1.4400	
2	C3	3	C3		110.1000	0.7000	
2	3	C3	O3		103.1000	0.4500	
					[g]		
3	00	3	00		0.1200		
3	H3	3	00		0.0900		
					[h]	[i]	[j]
4	1	2	3	H3	0.0000	0.0000	0.0000
4	1	2	3	C3	0.0000	0.0000	0.0000
4	H3	3	2	C3	0.0000	0.0000	0.0000
4	C3	3	2	C3	0.0000	0.0000	0.0000
4	H1	C3	2	3	0.0393	0.0151	0.8602
4	H1	C3	3	2	0.0009	0.0005	−0.2707
4	C3	2	3	Lp	−3.2092	5.0672	2.4880
4	H1	C3	3	Lp	0.0000	0.0000	0.0000
4	H1	C3	3	H3	0.0000	0.0000	0.2500
4	1	2	3	Lp	0.0000	0.0000	0.0000
4	C3	3	2	C2	0.0000	0.0000	0.0000
4	C2	2	3	Lp	−3.2092	5.0672	2.4880
4	C2	C2	2	3	1.8000	−1.6000	−1.4000
4	C2	C2	2	1	0.0000	0.0000	0.0000
4	C3	C3	3	2	0.0000	0.0000	0.0000
4	O3	C3	3	C3	−0.3000	0.0000	0.0000
4	3	C3	O3	C3	−0.2000	0.0000	0.0000
4	C3	C3	3	C3	−0.1000	0.3650	0.8550
4	H1	C3	3	C3	0.0000	0.0000	0.0000
4	C3	C3	3	Lp	0.0000	0.0000	0.0000
4	C3	C3	C3	3	0.0500	0.2000	0.4500
4	H1	C3	C3	3	−0.0750	0.0000	0.2750
4	C2	C3	C3	3	0.0000	0.0000	0.0900
4	C2	C3	3	2	0.0000	0.0000	0.0000
4	C2	C3	3	C3	0.0000	0.0000	0.2000

[a] Notation: Substructure atoms: 1 = O2 = O=, 2 = S1 = S, 3 = N3 = sp^3 N; H1 = H(–C); H3 = H(–N); C2 = sp^2 C, C3 = sp^3 C; O3 = O–; Lp = lone pair. [b] Bond length (Å). [c] Stretching constant (mdyn/Å). [d] Bond dipole moment (Debye). [e] Bond angle (°). [f] Bending constant (mdyn/rad^2). [g] Stretch-bend constant. [h] V_1 (kcal mol^{-1}). [i] V_2 (kcal mol^{-1}). [j] V_3 (kcal mol^{-1}).

0947-6539/96/0206-0650 $ 15.00+.25/0 Chem. Eur. J. 1996, 2, No. 6

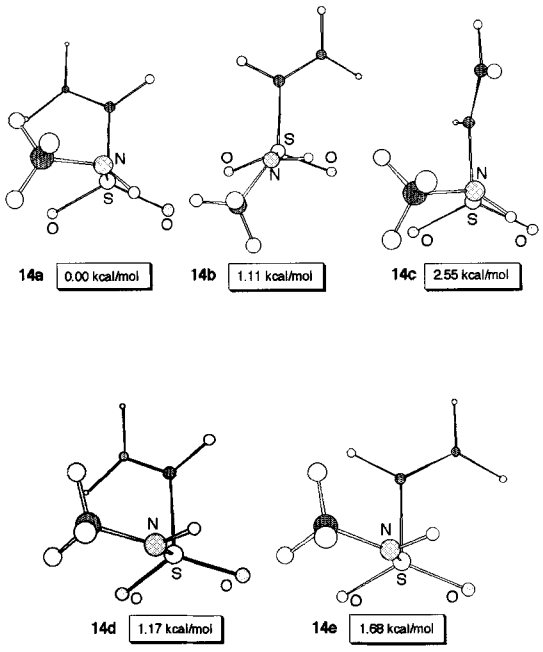

Fig. 12. Ab initio calculated conformers for $CH_2=CH-SO_2NHMe$ (**14**) and relative energies.

Table 6. Ab initio and force-field (FF) calculated relative energies and C=C–S–N dihedral angles of conformers **14a–e**. Torsional parameters $V_1 = 1.8$, $V_2 = -1.6$, $V_3 = -1.4$ are used for the $C(sp^2)=C(sp^2)-S-N$ torsion.

	Relative Energies (kcal mol^{-1})		C=C–S–N (°)	
	Ab initio	FF	Ab initio	FF
14a	0.00	0.00	−119	−115
14b	1.11	0.10	+119	+116
14c	2.55	2.57	+14	+11
14d	1.17	1.24	−113	−115
14e	1.68	1.39	+113	+115

provide a qualitative pictorial view of the low-energy conformers and match the pictures from the calculations with the spectroscopic data. Nevertheless, it is interesting to observe that in most cases the calculations correctly predict both the size of the hydrogen-bonded ring and its relative importance in agreement with the experimental data in solution (see discussion above).

Vs-peptides **9**, **10**, **12**, and **13** were subjected to the calculations; simplified structures in which all R substituents were replaced by methyl groups were used (Fig. 3, $R^1 = R^2 = R^3 = R^4 = Me$). The ratios of the various hydrogen-bonded and non-hydrogen-bonded conformational families are shown in Table 7. In the case of vs-dipeptide **9**, the predicted lowest-energy conformation is the fourteen-membered-ring hydrogen-bonded conformation (H9–O=C) found experimentally in solution (Fig. 13). In the case of vs-dipeptide **10**, the predicted lowest energy conformation is a doubly hydrogen-bonded conformation where both the fourteen-membered ring (H9–O=S hydrogen bonding) and the twelve-membered ring (H1–O=S) found experimentally in solution are present (Fig. 14). The calculations suggest that the twelve- and fourteen-membered-ring hydrogen-bonded conformations and the non-hydrogen-bonded conformations are all relevant for this compound, as found experimentally by the VT-NMR data (competition between various hydrogen-bonding networks), and IR data (equilibration between hydrogen-bonded and non-hydrogen-bonded states).

In the case of vs-tripeptide **12**, the predicted lowest-energy conformation is a fourteen-membered-ring hydrogen-bonded conformer (H9–O=C) (Fig. 15). The calculations suggest that both the fourteen-membered-ring conformations (H9–C=O and H13–S=O) are important, in agreement with the experimental data in solution. The calculations overestimate the population of conformers involving H1 in hydrogen bonds (H1–O=S, seventeen-membered ring) in clear contradiction to the spectroscopic data discussed above.

Table 7. Calculated percentages of the various hydrogen-bonded and non-hydrogen-bonded families of conformers within 2.0 kcal mol^{-1} (Boltzmann distribution at 298 K) for vs-peptides **9**, **10**, **12**, and **13** ($R^1 = R^2 = R^3 = R^4 = Me$); H-bond type in parentheses.

Conformers	**9**	**10**	**12**	**13**
non-hydrogen-bonded	7.9	37.8	4.3	0.5
14-membered-ring hydrogen-bonded	74.7 (H9–O=C)	26.0 (H9–O=S)	39.2 (H9–O=C)	5.6 (H9–O=C)
12-membered-ring hydrogen-bonded	8.7 (H1–O=S)	5.7 (H1–O=S)	–	–
12- and 14-membered-ring hydrogen-bonded	8.7 (H9–O=C) (H1–O=S)	30.5 (H9–O=S) (H1–O=S)	5.2 (H9–O=C) (H5–O=S)	–
17-membered-ring hydrogen-bonded	–	–	25.1 (H1–O=S)	–
19-membered-ring hydrogen-bonded	–	–	5.7 (H13–O=C)	3.9 (H13–O=C)
14- and 14-membered-ring hydrogen-bonded	–	–	13.4 (H9–O=C) (H13–O=S)	45.1 (H9–O=C) (H17–O=S)
14- and 19-membered-ring hydrogen-bonded	–	–	–	4.9 (H9–O=C) (H17–O=S)
14- and 22-membered-ring hydrogen-bonded	–	–	–	13.6 (H9–O=C) (H1–O=S)
various hydrogen-bonded rings (12-, 14-, 17-, 19- combinations)	–	–	7.1	–
various hydrogen-bonded rings (12-, 14-, 17-,19-, 22- combinations)	–	–	–	26.4

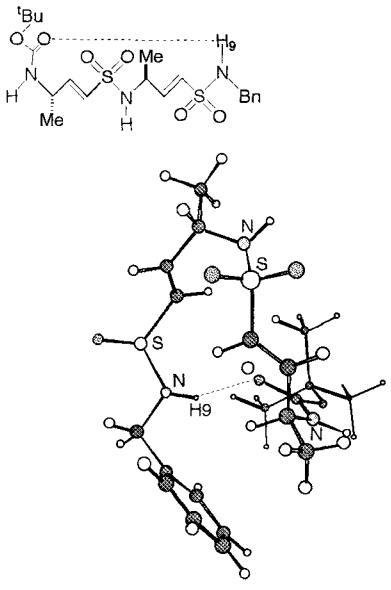

Fig. 13. Lowest-energy conformation (FF calculations) of vs-dipeptide **9**, $R^1 = R^2 = Me$, X = Boc. H9–O=C hydrogen-bonding distance = 1.94 Å. N–H9–O(=C) = 140.2°, (N–)H9–O=C = 135.8°.

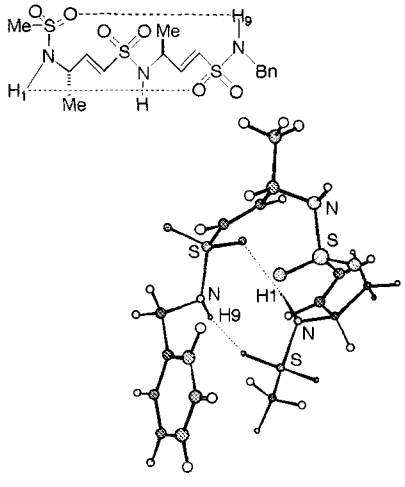

Fig. 14. Lowest-energy conformation (FF calculations) of vs-dipeptide **10**, $R^1 = R^2 = Me$, X = SO_2Me. H9–O=S hydrogen-bonding distance = 2.27 Å. N–H9–O(=S) = 169.9°, (N–)H9–O=S = 103.5°. H1–O=S hydrogen-bonding distance = 2.08 Å. N–H1–O(=S) = 149.4°, (N–)H1–O=S = 121.3°.

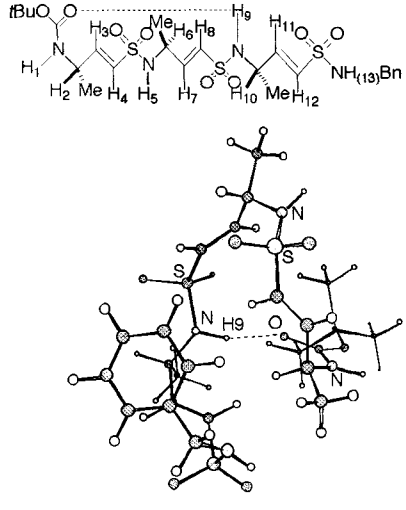

Fig. 15. Lowest-energy conformation (FF calculations) of vs-tripeptide **12**, $R^1 = R^2 = R^3 = Me$, X = NHBn. H9–O=C hydrogen-bonding distance = 1.93 Å. N–H9–O(=C) = 163.0°, (N)H9–O=C = 158.0°.

In the case of vs-tetrapeptide **13**, the predicted lowest-energy conformation is a doubly hydrogen-bonded conformer where both the fourteen-membered hydrogen-bonded ring involving the Boc carbonyl group (H9–O=C) and that involving the terminal benzyl sulfonamide proton (H17–O=S) are present (Fig. 16). The calculations suggest that the fourteen-membered-ring hydrogen-bonding motif becomes increasingly important in more structurally complex substrates.

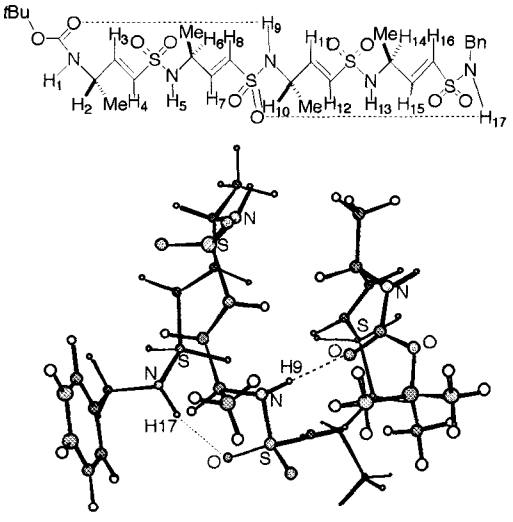

Fig. 16. Lowest-energy conformation (FF calculations) of vs-tetrapeptide **13**, $R^1 = R^2 = R^3 = R^4 = Me$, X = NHBn. H9–O=C hydrogen-bonding distance = 1.90 Å. N–H9–O(=C) = 154.6°, (N–)H9–O=C = 157.3°. H17–O=S hydrogen-bonding distance is 2.04 Å. N–H17–O(=S) = 159.0°, (N–)H17–O=S = 127.5°.

Conclusion

We have investigated the conformational preferences of chiral vinylogous aminosulfonic acids (vs-amino acids) and of the corresponding oligomers (vs-peptides) by a combination of X-ray crystallography, variable-temperature (VT) ^{1}H NMR spectroscopy, FT-IR spectroscopy, and NOE experiments. The major source of conformational freedom in the monomers is the rotation around the C–C bond connecting the double bond with the allylic stereocenter (N–C*–C=C). The allylic conformational preferences can be altered in the oligomers by the formation of secondary structures enforced by hydrogen bonding. Twelve-membered-ring hydrogen bonding is detected in the crystal structure of vs-dipeptide **9**, while fourteen-membered-ring hydrogen bonding is the most common folding pattern for the oligomers in chloroform solution. With little competition from different hydrogen-bonding networks, the fourteen-membered ring is largely favored and strengthened by a more linear N–H–O angle. The experimental results were complemented by computer modeling: the calculations correctly predict both the size of the hydrogen-bonded ring and its relative importance.

Experimental Section

Computer modeling: A Goodman–Still systematic pseudo-Monte-Carlo search [15a], part of the BATCHMIN-MacroModel 4.5 molecular mechanics program [15b], was used for the conformational search on a Silicon Graphics Iris workstation. The conformers were minimized in chloroform with the GB/SA model included in BATCHMIN [15c]. For this solvation model, molecular electrostatics calculations were carried out with a constant dielectric treatment (molecular dielectric

0947-6539/96/0206-0652 $ 15.00+.25/0 Chem. Eur. J. 1996, 2, No. 6

constant $\varepsilon_{mol} = 1.0$). A solvent dielectric constant ε_{solv} of 4.8 was used for chloroform. The force-field calculations were carried out by means of the MM2* force field implemented in the MacroModel program [15b], augmented by the sulfonamide substructure described above. MM2* resembles the Allinger MM2 force field, but electrostatic effects and improper torsion are treated differently in the MacroModel version.

The low energy conformations (within 2.0 kcal mol^{-1} from the global minimum) were analyzed with respect to their hydrogen-bonding pattern. Hydrogen-bonding populations were estimated by analyzing the geometry around the acceptor (O) and the donor (H) atoms: a hydrogen bond was counted as present if the (N)H–O distance was ≤ 2.5 Å, the N–H–O angle was $\geq 120°$ and the H–O=C (or H–O=S) angle was $\geq 90°$ [15d,16].

Crystal structure analysis (Table 8 [17]): Unit cell parameters and intensity data were obtained with an Enraf–Nonius CAD-4 diffractometer and graphite monochromated $Cu_{K\alpha}$ radiation ($\lambda = 1.54184$ Å). Calculations were performed with SDP and MolEN software [18] on a MicroVax-3100 computer. The space groups were obtained by systematic extinctions and intensity statistics, and confirmed by the solution and refinement of the structures. The cases of space group $P1$ (**2** and **9**) are quite surprising, but any attempt to describe the crystal structures in a higher symmetry space group according to refs. [19] and [20] failed. Data were collected at room temperature by $\omega-2\theta$ scan type in the θ range 0–70°. Lone pair (lp), decay, and absorption [21] corrections were applied. The structures were solved by direct methods (MULTAN 80) [22]. All the non-hydrogen atoms were anisotropically refined by full-matrix least squares. The positions of all the hydrogen atoms were experimentally determined, but refined with success only in the case of **1** and, partially, in the case of **9** (amidic hydrogen atoms only). Atomic scattering factors were taken from reference [23].

Physical data:

L-Boc–vs-Ala–OMe (1): Crystallized from *n*-hexane/EtOAc 7:3; m.p. = 89–91 °C; $[\alpha]_D^{20} = -22.3°$ ($c = 1.0$, $CHCl_3$); ^{1}H NMR (300 MHz, $CDCl_3$, 300 K, TMS): $\delta = 1.33$ (d, ^3J(H,H) = 7.0 Hz, 3H; CH_3CH), 1.45 (s, 9H; [CH_3]$_3$C), 3.82 (s, 3H; CH_3OSO$_2$), 4.45 (m, 1H; CH$_3$CHN), 4.61 (d, ^3J(H,H) = 4.40 Hz, 1H; NH), 6.27 (dd, ^3J(H,H) = 15.10 Hz, ^4J(H,H) = 1.60 Hz, 1H; CH=CHSO$_3$), 6.86 (dd, ^3J(H,H) = 15.10 Hz, ^3J(H,H) = 4.97 Hz, 1H; CH=CHSO$_3$); ^{13}C NMR (50.28 MHz, $CDCl_3$, 300 K, TMS): $\delta = 19.61$ (CH_3), 28.15 ([CH_3]$_3$), 46.75 (CHN), 56.16 (OCH_3), 122.71 (CH=), 150.66 (CH=); $C_{10}H_{19}NO_5S$ (265.3): calcd C 45.27, H 7.22, N 5.28, S 12.08, O 30.15; found C 45.21, H 7.28, N 5.25.

L-Boc–vs-Val–OEt (2): Crystallized from *n*-hexane; m.p. = 53–55 °C; $[\alpha]_D^{20} = +3.15°$ ($c = 1.0$, $CHCl_3$); ^{1}H NMR (300 MHz, $CDCl_3$, 300 K, TMS): $\delta = 0.95$ (d, ^3J(H,H) = 6.4 Hz, 3H; CH_3CH), 1.36 (t, ^3J(H,H) = 7.5 Hz, 3H; CH_3CH$_2$OSO$_2$), 1.44 (s, 9H; [CH_3]$_3$C), 1.88 (m, ^3J(H,H) = 6.4 Hz, 1H; [CH$_3$]$_2$CH), 4.15 (q, ^3J(H,H) = 7.5 Hz, 2H; CH$_3$CH_2OSO$_2$,), 4.20 (m, 1H; H2), 4.55 (br, 1H; H1), 6.32 (dd, ^3J(H,H) = 14.65 Hz, ^4J(H,H) = 1.90 Hz, 1H; H4), 6.80 (dd, ^3J(H,H) = 14.65 Hz, ^3J(H,H) = 4.88 Hz, 1H; H3); ^{13}C NMR (50.28 MHz, $CDCl_3$, 300 K, TMS): $\delta = 14.69$ (CH_3), 17.95 (CH_3), 18.74 (CH_3), 28.14 ([CH_3]$_3$), 31.78 (CH), 56.38 (CHN), 66.81 (CH_2), 125.16 (CH=), 147.63 (CH=); $C_{13}H_{25}NO_5S$ (307.4): calcd C 50.79, H 8.20, N 4.56, S 10.41, O 26.04; found C 50.71, H 8.25, N 4.52.

L-Boc–vs-Phe–OMe (3): Crystallized from *n*-hexane/EtOAc 70:30; m.p. = 115–117 °C; $[\alpha]_D^{20} = +10.76°$ ($c = 1.05$, $CHCl_3$); ^{1}H NMR (300 MHz, $CDCl_3$, 300 K, TMS): $\delta = 1.42$ (s, 9H; [CH_3]$_3$), 2.95 (d, ^3J(H,H) = 6.63 Hz, 2H; CH_2Ph), 3.73 (s, 3H; CH_3OSO_2), 4.37 (m, 1H; H2), 4.47 (m, 1H; H1), 6.24 (dd, ^3J(H,H) = 14.65 Hz, ^4J(H,H) = 1.27 Hz, 1H; H4), 6.83 (dd, ^3J(H,H) = 14.65 Hz, ^3J(H,H) = 5.37 Hz, 1H; H3), 7.10–7.35 (m, 5H; ArH); ^{13}C NMR (50.28 MHz, $CDCl_3$, 300 K, TMS): $\delta = 28.84$ ([CH_3]$_3$), 40.88 (CH_2Ph), 52.71 (CHN), 56.79 (OCH_3), 124.64 (CH=), 127.83 (Ar), 129.41 (Ar), 129.87 (Ar), 136.28 (Ar), 149.35 (CH=), 155.40 (CO); $C_{16}H_{23}NO_5S$ (341.4): calcd C 56.29, H 6.79, N 4.10, S 9.39, O 23.43; found 56.35, H 6.82, N 4.07.

L-Boc–vs-Leu–OMe (4): Crystallized from *n*-hexane/EtOAc 95:5; m.p. = 59–61 °C; $[\alpha]_D^{20} = -15.36°$ ($c = 1.0$, $CHCl_3$); ^{1}H NMR (300 MHz, $CDCl_3$, 300 K, TMS): $\delta = 0.95$ (d, ^3J(H,H) = 6.6 Hz, 6H; [CH_3]$_2$CH), 1.40–1.54 (m, 2H; iPr-CH_2), 1.45 (s, 9H; [CH_3]$_3$C), 1.64 (m, 1H; Me$_2$CH), 3.81 (s, 3H; CH_3OSO$_2$), 4.40 (m, 1H; CHN), 4.50 (brd, 1H; NH), 6.28 (dd, ^3J(H,H) = 15.10 Hz, ^4J(H,H) = 1.20 Hz, 1H; CH=CHSO$_3$), 6.79 (dd, ^3J(H,H) = 16.10 Hz, ^3J(H,H) = 5.37 Hz, 1H; CH=CHSO$_3$); ^{13}C NMR (50.28 MHz, $CDCl_3$, 300 K, TMS): $\delta = 21.77$ (CH_3), 22.58 (CH_3), 24.56 (CH), 28.18 ([CH_3]$_3$), 42.61 (CH_2), 49.42 (CHN), 56.12 (CH_3), 122.81 (CH=), 150.30 (CH=); $C_{13}H_{25}NO_5S$ (307.4): calcd C 50.79, H 8.20, N 4.56, S 10.43, O 26.02; found C 50.72, H 8.25, N 4.50.

L-Boc–vs-Ala–NHBn (5): ^{1}H NMR (300 MHz, $CDCl_3$, 300 K, TMS): $\delta = 1.25$ (d, ^3J(H,H) = 6.78 Hz, 3H; CH_3CH), 1.46 (s, 9H; [CH_3]$_3$C), 4.21 (d, 2H; NHCH_2Ph), 4.36 (m, 1H; NCHCH$_3$), 4.45 (d, ^3J(H,H) = 7.3 Hz, 1H; NHCH), 4.45 (m, 1H; SO$_2$NHCH$_2$), 6.24 (dd, ^3J(H,H) = 15.1 Hz, ^4J(H,H) = 1.3 Hz, 1H; CH=CHSO$_2$), 6.67 (dd, ^3J(H,H) = 4.65 Hz, ^3J(H,H) = 15.1 Hz, 1H; CH=CHSO$_2$), 7.35 (m, 5H; ArH); $C_{16}H_{24}N_2O_4S$ (340.4): calcd C 56.45, H 7.11, N 8.23, S 9.42, O 18.80; found C 56.43, H 7.16, N 8.20.

L-MeSO$_2$–vs-Ala–NHBn (6): ^{1}H NMR (300 MHz, $CDCl_3$, 300 K, TMS): $\delta = 1.34$ (d, ^3J(H,H) = 7.1 Hz, 3H; CH_3CH), 2.96 (s, 3H; CH_3SO$_2$), 4.23 (d, ^3J(H,H) = 6.1 Hz, 3H; NCH_2Ph + NHCH), 4.20 (d, ^3J(H,H) = 8.3 Hz, 1H; MeSO$_2$NH), 4.58 (t, ^3J(H,H) = 6.1 Hz, 1H; SO$_2$NHBn), 6.38 (dd, ^3J(H,H) = 15.1 Hz, ^4J(H,H) = 1.6 Hz, 1H; CH=CHSO$_2$), 6.66 (dd, ^3J(H,H) = 5.13 Hz, ^3J(H,H) = 15.1 Hz, 1H; CH=CHSO$_2$), 7.35 (m, 5H; ArH); $C_{12}H_{18}N_2O_4S_2$ (318.4): calcd C 45.27, H 5.70, N 8.80, S 20.14, O 20.10; found C 45.22, H 5.75, N 8.78.

Table 8. Crystal structure analyses.

	3	**2**	**1**	**9**
formula	$C_{16}H_{23}NO_5S$	$C_{13}H_{25}NO_5S$	$C_{10}H_{19}NO_5S$	$C_{22}H_{35}N_3O_6S_2$
FW	341.42	307.40	265.33	501.67
system	trigonal	triclinic	monoclinic	triclinic
space group	$R3$ (no. 146)	$P1$ (no. 1)	$P2_1$ (no. 4)	$P1$ (no. 1)
a (Å)	29.142(6)	5.318(6)	7.944(2)	5.599(1)
b (Å)	29.142(6)	6.728(4)	9.620(1)	9.193(2)
c (Å)	5.419(1)	12.292(9)	9.948(3)	13.672(3)
α (°)	90	78.43(7)	90	73.34(2)
β (°)	90	88.44(6)	112.98(1)	88.00(2)
γ (°)	120	84.66(6)	90	75.37(2)
V (Å^3)	3986(1)	429.0(7)	699.9(3)	651.8(3)
ρ_{calcd} (Mg m^{-3})	1.281	1.190	1.259	1.278
absor. coeff. (1 mm^{-1})	1.79	1.79	2.12	2.15
cryst. size (mm)	0.4 × 0.1 × 0.1	0.1 × 0.1 × 0.08	0.5 × 0.1 × 0.1	0.4 × 0.4 × 0.3
no. refl. meas	4941	2505	1876	2616
no. unique refl.	3256	1616	1418	2348
no. refl. obs.	2832	1528	1256	2296
criterion for obs.	$I > 2\sigma(I)$	$I > 2\sigma(I)$	$I > 2\sigma(I)$	$I > 2\sigma(I)$
T_{min}, T_{max}	0.932, 0.996	0.903, 0.996	0.928, 1.000	0.961, 0.999
variation obs. stand.	−4.5%	−7.1%	−2.3%	−5.2%
decay correction	linear	linear	linear	linear
refinement type	on F	on F	on F	on F
R	0.034	0.056	0.053	0.037
R_w	0.034	0.055	0.049	0.038
no. refined param.	299	181	154	306
weighting scheme (w =)	1	$1/[\sigma(F)]^2$	$1/[\sigma(F)]^2$	$1/[\sigma(F)]^2$
$(\Delta/\rho)_{min}$ (e Å^{-3})	−0.09	−0.12	−0.15	−0.12
$(\Delta/\rho)_{max}$ (e Å^{-3})	0.10	0.18	0.10	0.12

L-Boc-vs-Ala-L-vs-Val-NHBn (9): Crystallized from *n*-hexane/EtOAc 50:50; m.p. = 134–136 °C; $[\alpha]_D^{20} = -7.9°$ ($c = 1.01$, $CHCl_3$); ^{1}H NMR (300 MHz, $CDCl_3$, 300 K, TMS): $\delta = 0.92$ (d, $^3J(H,H) = 6.84$ Hz, 3H; CH_3), 0.96 (d, $^3J(H,H) = 6.84$ Hz, 3H; CH_3), 1.21 (d, $^3J(H,H) = 7.08$ Hz, 3H; CH_3), 1.44 (s, 9H; $[CH_3]_3$), 3.86 (br, 1H; H6), 4.15 (b, 1H; H2), 4.20 (br, 1H; H5), 4.2 (d, $^3J(H,H) = 5.2$ Hz, 2H; CH_2Ph), 4.59 (br, 1H; H1), 5.96 (br, 1H; H9), 6.12 (d, $^3J(H,H) = 14.65$ Hz, 1H; H8), 6.31 (d, $^3J(H,H) = 15.63$ Hz, 1H; H4), 6.46 (dd, $^3J(H,H) = 5.86$ Hz, $^3J(H,H) = 14.65$ Hz, 1H; H7), 6.57 (dd, $^3J(H,H) = 15.63$ Hz, $^3J(H,H) = 4.88$ Hz, 1H; H3); ^{13}C NMR (50.28 MHz, $CDCl_3$, 300 K, TMS): $\delta = 18.001$ (CH_3), 18.724 (CH_3), 19.536 (CH_3), 28.215 ($[CH_3]_3$), 32.361 (CH), 46.524 (CH), 46.954 (CH_2), 59.330 (CH), 127.663, 127.901, 128.269, 128.547, 130.366, 141.986, 145.450; $C_{22}H_{35}N_3O_6S_2$ (501.7): calcd C 52.67, H 7.03, N 8.38, O 19.14, S 12.78; found C 52.62, H 7.09, N 8.32.

L-$MeSO_2$-vs-Ala-L-vs-Val-NHBn (10): ^{1}H NMR (300 MHz, $CDCl_3$, 300 K, TMS): $\delta = 0.93$ (d, $^3J(H,H) = 6.84$ Hz, 6H; CH_3Val), 1.36 (d, $^3J(H,H) = 7.8$ Hz, 3H; CH_3Ala), 1.85 (m, 1H; $CH(CH_3)_2$), 2.95 (s, 3H; CH_3SO_2), 3.8 (m, 1H; H6), 4.1 (q, $^3J(H,H) = 7.8$ Hz, 1H; H2), 4.19–4.26 (q, $^3J(H,H) = 7.80$ Hz, 2H; CH_2), 4.43 (d, $^3J(H,H) = 8.8$ Hz, 1H; H5), 5.02 (d, $^3J(H,H) = 8.89$ Hz, 1H; H1), 5.23 (t, $^3J(H,H) = 5.86$ Hz, 1H; H9), 6.31 (d, $^3J(H,H) = 15.63$ Hz, 1H; H4), 6.36 (d, $^3J(H,H) = 14.65$ Hz, 1H; H8), 6.45 (dd, $^3J(H,H) = 15.63$ Hz, $^3J(H,H) = 6.84$ Hz, 1H; H3), 6.68 (dd, $^3J(H,H) = 4.88$ Hz, $^3J(H,H) = 14.65$ Hz, 1H; H7), 7.25 (s, 5H; Ph); $C_{18}H_{29}N_3O_6S_3$ (479.6): calcd C 45.08, H 6.09, N 8.76, S 20.05, O 20.01; found C 45.05, H 6.13, N 8.70.

L-Boc-vs-Phe-L-vs-Ala-L-vs-Val-OEt (11): ^{1}H NMR (300 MHz, $CDCl_3$, 300 K, TMS): $\delta = 0.96$ (d, $^3J(H,H) = 7.5$ Hz, 3H; CH_3Val), 0.98 (d, $^3J(H,H) = 7.0$ Hz, 3H; CH_3Val), 1.33 (d, $^3J(H,H) = 6.5$ Hz, 3H; CH_3Ala), 1.39 (s, 9H; $[CH_3]_3C$), 1.41 (t, $^3J(H,H) = 7.0$ Hz, 3H; $CH_3CH_2OSO_2$), 1.88 (m, 1H; Me_2CH), 2.82 (dd, $^2J(H,H) = 14.0$ Hz, $^3J(H,H) = 7.0$ Hz, 1H; CHHPh), 3.01 (d, $^2J(H,H) = 14.0$ Hz, 1H; CHHPh), 3.91 (q, $^3J(H,H) = 7.5$ Hz, 1H; H10), 4.19 (m, 1H; H6), 4.25 (m, 2H; CH_2OSO_2), 4.34 (d, $^3J(H,H) = 7.8$ Hz, 1H; H5), 4.62 (m, 2H; H2 + H1), 5.80 (d, $^3J(H,H) = 8.8$ Hz, 1H; H9), 6.21 (d, $^3J(H,H) = 15.0$ Hz, 1H; H4), 6.29 (d, $^3J(H,H) = 15.3$ Hz, 1H; H12), 6.39 (dd, $^3J(H,H) = 15.4$ Hz, 1H; H8), 6.46 (dd, $^3J(H,H) = 15.4$ Hz, $^3J(H,H) = 4.64$ Hz, 1H; H7), 6.75 (dd, $^3J(H,H) = 15.3$ Hz, $^3J(H,H) = 7.57$ Hz, 1H; H11), 6.83 (dd, $^3J(H,H) = 15.0$ Hz, $^3J(H,H) = 4.0$ Hz, 1H; H3), 7.25 (s, 5H; Ph); ^{13}C NMR (50.28 MHz, $CDCl_3$, 300 K, TMS): $\delta = 14.89$ (CH_3), 18.19 ($2CH_3$), 18.73 (CH_3), 28.19 ($[CH_3]_3$), 32.48 (CH), 39.79 (CH_2Ph), 49.23 (CHN), 52.11 (CHN), 59.89 (CHN), 67.09 (OCH_2), 126.67, 127.01, 128.65, 128.72, 129.20, 130.05, 143.00, 144.87, 146.08, 155.32 (C=O); $C_{27}H_{43}N_3O_9S_3$ (649.8): calcd C 49.90, H 6.67, N 6.47, S 14.80, O 22.16; found C 49.80, H 6.70, N 6.46.

L-Boc-vs-Phe-L-vs-Ala-L-vs-Val-NHBn (12): ^{1}H NMR (300 MHz, $CDCl_3$, 300 K, TMS): $\delta = 0.93$ (d, $^3J(H,H) = 6.84$ Hz, 6H; CH_3Val), 1.23 (d, $^3J(H,H) = 7.0$ Hz, 3H; CH_3Ala), 1.37 (s, 9H; $[CH_3]_3C$), 1.81 (m, 1H; Me_2CH), 2.82 (dd, $^3J(H,H) = 6.8$ Hz, $^2J(H,H) = 13.6$ Hz, 1H; CHCHHPh), 3.0 (dd, $^3J(H,H) = 3.0$ Hz, $^2J(H,H) = 13.6$ Hz, 1H; CHCHHPh), 3.83 (q, 1H; H10), 3.91 (m, 1H; H6), 4.26 (d, $^3J(H,H) = 6.8$ Hz, 2H; NCH_2Ph), 4.46 (d, $^3J(H,H) = 7.8$ Hz, 1H; H5), 4.58 (m, 2H; H2 + H1), 5.24 (t, $^3J(H,H) = 6.8$ Hz, 1H; H13), 5.5 (d, $^3J(H,H) = 9.7$ Hz, 1H; H9), 6.13 (d, $^3J(H,H) = 15.63$ Hz, 1H; H8), 6.18 (d, $^3J(H,H) = 15.63$ Hz, 1H; H4), 6.23 (d, $^3J(H,H) = 15.63$ Hz, 1H; H12), 6.38 (dd, $^3J(H,H) = 15.63$ Hz, $^3J(H,H) = 5.86$ Hz, 1H; H7), 6.53 (d, $^3J(H,H) = 15.63$ Hz, $^3J(H,H) = 7.8$ Hz, 1H; H11), 6.88 (dd, $^3J(H,H) = 15.63$ Hz, $^3J(H,H) = 3.9$ Hz, 1H; H3), 7.1–7.4 (m, 10H; ArH); ^{13}C NMR (50.28 MHz, $CDCl_3$, 300 K, TMS): $\delta = 18.014$ (CH_3), 18.780 (CH_3), 28.158 ($[CH_3]_3$), 40.1 (CH_2), 46.895 (NCH_2Ph), 49.280 (CHN), 126.90, 127.8, 127.940, 128.585, 128.662, 129.241, 130.546, 142.086, 144.881; $C_{32}H_{46}N_4O_8S_3$ (710.9): calcd C 54.06, H 6.52, N 7.88, S 13.53, O 18.00; found C 54.00, H 6.59, N 7.86.

L-Boc-vs-Leu-L-vs-Phe-L-vs-Ala-L-vs-Val-NHBn (13): ^{1}H NMR (300 MHz, $CDCl_3$, 300 K, TMS): $\delta = 0.92$ (d, $^3J(H,H) = 6.6$ Hz, 6H; CH_3Val), 1.25–1.35 (m, 5H; CH_3Ala + iPrCH_2), 1.45 (s, 9H; $[CH_3]_3C$), 1.64 (m, 1H; Me_2CHCH_2), 1.83 (m, 1H; Me_2CH), 2.76 (dd, $^3J(H,H) = 9$ Hz, $^2J(H,H) = 14.1$ Hz, 1H; CHCHHPh), 3.0 (dd, $^3J(H,H) = 4.9$ Hz, $^2J(H,H) = 14.1$ Hz, 1H; CHCHHPh), 3.82 (m, 1H; H14), 4.04 (m, 1H; H10), 4.1–4.3 (m, 2H; H6 + H2), 4.2 (d, $^3J(H,H) = 6.21$ Hz, 2H; NCH_2Ph), 4.4 (d, $^3J(H,H) = 8.0$ Hz, 1H; H5), 4.65 (d, $^3J(H,H) = 8.0$ Hz, 1H; H1), 4.94 (d, $^3J(H,H) = 8.8$ Hz, 1H; H13), 5.35 (m, 1H; H17), 5.60 (d, $^3J(H,H) = 7.3$ Hz, 1H; H9), 5.94 (d, $^3J(H,H) = 15.1$ Hz, 1H; H8), 6.23 (d, $^3J(H,H) = 15.0$ Hz, 1H; H16), 6.39 (d, $^3J(H,H) = 15.1$ Hz, 1H; H4), 6.45 (dd, $^3J(H,H) = 6.3$ Hz, 1H; H11), 6.52 (dd, $^3J(H,H) = 6.84$ Hz, $^3J(H,H) = 15.0$ Hz, 1H; H15), 6.61 (dd, $^3J(H,H) = 5.0$ Hz, $^3J(H,H) = 15.1$ Hz, 1H; H3), 6.64 (dd, $^3J(H,H) = 5.86$ Hz, $^3J(H,H) = 15.1$ Hz, 1H; H7), 7.2–7.4 (m, 10H; ArH); ^{13}C NMR (50.28 MHz, $CDCl_3$, 300 K, TMS): $\delta = 18.014$ (CH_3), 18.715 (CH_3), 20.944 (CH_3), 21.651 (CH_3), 22.821 (CH_3), 24.582 (CH), 28.225 ($[CH_3]_3$), 32.535 (CH), 40.264 (CH_2Ph), 43.077 (CH_2), 46.925 (NCH_2Ph), 49.060 (NCH), 49.559 (NCH), 55.208 (NCH), 59.363 (NCH), 126.815, 127.269, 127.870, 127.975, 128.684, 128.836, 129.705, 129.901, 130.267, 130.656, 142.020, 143.490, 143.767, 146.483; $C_{39}H_{59}N_5O_{10}S_4$ (886.2): calcd C 52.86, H 6.71, N 7.90, S 14.47, O 18.05; found C 52.80, H 6.79, N 7.85.

Acknowledgments: The authors thank Dr Laura Belvisi, Dr Anna Bernardi, and Maria B. Villa for assistance with the computational section. We are grateful to Pharmacia and Upjohn (Milano) for financial support.

Received: September 14, 1995 [F213]

[1] A. Giannis, T. Kolter, *Angew. Chem.* **1993**, *105*, 1303–1326; *Angew. Chem. Int. Ed. Engl.* **1993**, *32*, 1244–1267.

[2] J. Gante, *Angew. Chem.* **1994**, *106*, 1780–1802; *Angew. Chem. Int. Ed. Engl.* **1994**, *33*, 1699–1720.

[3] a) W. J. Moree, G. A. van der Marel, R. M. J. Liskamp, *Tetrahedron Lett.* **1992**, *33*, 6389–6392; b) W. J. Moree, G. A. van der Marel, R. M. J. Liskamp, *ibid.* **1991**, *32*, 409–412; c) W. J. Moree, L. C. van Gent, G. A. van der Marel, R. M. J. Liskamp, *Tetrahedron* **1993**, *49*, 1133–1150; d) W. J. Moree, G. A. van der Marel, R. M. J. Liskamp, *J. Org. Chem.* **1995**, *60*, 5157–5169; e) A. Calcagni, E. Gavuzzo, F. Mazza, F. Pinnen, G. Pochetti, D. Rossi, *Gazz. Chim. Ital.* **1992**, *122*, 17–23; f) H. R. Kricheldorf, E. Leppert, *Synthesis* **1976**, 43–45; g) G. Pagani Zecchini, M. Paglialunga Paradisi, I. Torrini, G. Lucente, E. Gavuzzo, F. Mazza, G. Pochetti, *Tetrahedron Lett.* **1991**, *32*, 6779–6782; h) G. Luisi, A. Calcagni, F. Pinnen, *ibid.* **1993**, *34*, 2391–2392; i) R. M. J. Liskamp, *Angew. Chem.* **1994**, *106*, 661–664; *Angew. Chem. Int. Ed. Engl.* **1994**, *33*, 633–636; j) C. H. Levenson, R. B. Meyer, Jr., *J. Med. Chem.* **1984**, *27*, 228–232; k) R. Guégan, J. Diaz, C. Cazaubon, M. Beaumont, C. Carlet, J. Clément, H. Demarne, M. Mellet, J.-P. Richaud, D. Segondy, M. Vedel, J.-P. Gagnol, R. Roncucci, B. Castro, P. Corvol, G. Evin, B. P. Roques, *ibid.* **1986**, *29*, 1152–1159; l) H. Mazdiyasni, D. B. Konopacki, D. A. Dickman, T. M. Zydowsky, *Tetrahedron Lett.* **1993**, *34*, 435–438.

[4] a) M. Frankel, P. Moses, *Tetrahedron* **1960**, *9*, 289–294; b) W. F. Gilmore, H.-J. Lin, *J. Org. Chem.* **1978**, *43*, 4535–4537; c) G. R. Moe, L. M. Sayre, P. S. Portoghese, *Tetrahedron Lett.* **1981**, *22*, 537–540; d) B. Garrigues, M. Mulliez, *Synthesis* **1988**, 810–813; e) D. Merricks, P. G. Sammes, E. R. H. Walker, K. Henrick, M. M. McPartlin, *J. Chem. Soc. Perkin 1* **1991**, 2169–2176.

[5] a) C. Gennari, B. Salom, D. Potenza, A. Williams, *Angew. Chem.* **1994**, *106*, 2181–2183; *Angew. Chem. Int. Ed. Engl.* **1994**, *33*, 2067–2069; b) C. Gennari, B. Salom, D. Potenza, Italian Patent Application 17 May **1994**, N. MI94 A 000989; PCT Int. Appl. EP 95-01788, 11 May **1995**; c) C. Gennari, H. P. Nestler, B. Salom, W. C. Still, *Angew. Chem.* **1995**, *107*, 1892–1893; *Angew. Chem. Int. Ed. Engl.* **1995**, *34*, 1763–1765; d) C. Gennari, H. P. Nestler, B. Salom, W. C. Still, *ibid.* **1995**, *107*, 1894–1896 and **1995**, *34*, 1765–1768.

[6] a) S. H. Gellman, G. P. Dado, G.-B. Liang, B. R. Adams, *J. Am. Chem. Soc.* **1991**, *113*, 1164–1173; b) G. P. Dado, S. H. Gellman, *ibid.* **1993**, *115*, 4228–4245; c) V. Dupont, A. Lecoq, J.-P. Mangeot, A. Aubry, G. Boussard, M. Marraud, *ibid.* **1993**, *115*, 8898–8906, and references therein; d) E. A. Gallo, S. H. Gellman, *ibid.* **1993**, *115*, 9774–9788; e) G. P. Dado, S. H. Gellman, *ibid.* **1994**, *116*, 1054–1062; f) T. S. Haque, J. C. Little, S. H. Gellman, *ibid.* **1994**, *116*, 4105–4106; g) R. R. Gardner, G.-B. Liang, S. H. Gellman, *ibid.* **1995**, *117*, 3280–3281; h) M. Paradisi Paglialunga, I. Torrini, G. Zecchini Pagani, G. Lucente, E. Gavuzzo, F. Mazza, G. Pochetti, *Tetrahedron* **1995**, *51*, 2379–2386.

[7] vs-AA-OH = vinylogous sulfonyl amino acid. Defined vinylogous sulfonyl amino-acid residues are described by the vs-prefix to the three-letter code of the corresponding amino acid; for example, vs-Ala = vinylogous sulfonyl alanyl.

[8] a) M. Nishio, Y. Umezawa, M. Hirota, Y. Takeuchi, *Tetrahedron* **1995**, *51*, 8665, and references cited therein; b) S. Paliwal, S. Geib, C. S. Wilcox, *J. Am. Chem. Soc.* **1994**, *116*, 4497–4498.

[9] The folding preferences in a solvent of this kind may be relevant for the binding of vs-peptides with proteins or other receptors in nonpolar situations (e.g., the interior of a biomembrane). Acetonitrile and DMSO, which are significantly more polar than chloroform, are known to severely disrupt intramolecular hydrogen bonding in amides (ref. [6]).

[10] A greater observed ^3J indicates an increased population of the CH2-eclipsed rotamer. On the basis of the Boltzmann distribution law, at lower temperatures the population of the more stable rotamer should rise. Thus, a greater observed H2–H3 coupling constant at lower temperatures indicates that the CH2-eclipsed rotamer (H–C*–C=C ca. 0°) is more stable, while a smaller H2–H3 coupling constant at lower temperatures indicates that the CN-eclipsed rotamer (N–C*–C=C ca. 0°) is more stable. See: a) B. W. Gung, M. S. Gerdeman, R. A. Fouch, M. A. Wolf, *J. Org. Chem.* **1994**, *59*, 4255–4261; b) B. W. Gung, J. P. Melnick, M. A. Wolf, J. A. Marshall, S. Beaudoin, *ibid.* **1994**, *59*, 5609–5613; c) B. W. Gung, M. A. Wolf, *ibid.* **1993**, *58*, 7038; d) B. W. Gung, J. P. Melnick, M. A. Wolf, A. King, *ibid.* **1995**, *60*, 1947.

[11] The concentration independence of δ(NH) values does not in principle allow one to distinguish between a lack of aggregation and the formation of an extremely stable aggregate (e.g., vs-dipeptide, vs-tripeptide, etc.). However, this seems unlikely. For a discussion of this possibility, see footnote 13 of ref. [6b] and footnote 16 of ref. [6f].

[12] a) J. B. Nicholas, R. Vance, E. Martin, B. J. Burke, A. J. Hopfinger, *J. Phys. Chem.* **1991**, *95*, 9803; b) J. Elguero, P. Goya, I. Rozas, J. Catalan, J. L. G. De Paz, *J. Mol. Struct. (Theochem)* **1989**, *184*, 115; c) R. D. Bindal, J. T. Golab, J. A. Katzenellenbogen, *J. Am. Chem. Soc.* **1990**, *112*, 7861; d) L. Belvisi, O. Carugo, G. Poli, *J. Mol. Struct.* **1994**, *318*, 189–202.

[13] M. J. Frisch, M. Head-Gordon, G. W. Trucks, J. B. Foresman, H. B. Schlegel, K. Raghavachari, M. A. Robb, J. S. Binkley, C. Gonzalez, D. J. Defrees, D. J. Fox, R. A. Whiteside, R. Seeger, C. F. Melius, J. Beker, R. L. Martin, L. R. Kahn, J. J. P. Stewart, S. Topiol, J. A. Pople, Gaussian, Pittsburgh, PA, **1990**.
[14] a) For a conformational analysis of vinylogous polypeptides, see: M. Hagihara, N. J. Anthony, T. J. Stout, J. Clardy, S. L. Schreiber, *J. Am. Chem. Soc.* **1992**, *114*, 6568–6570; b) for a conformational analysis of 1,2-diaminoethane diureas, see: J. S. Nowick, M. Abdi, K. A. Bellamo, J. A. Love, E. J. Martinez, G. Noronha, E. M. Smith, J. W. Ziller, *J. Am. Chem. Soc.* **1995**, *117*, 89–99.
[15] a) J. M. Goodman, W. C. Still, *J. Comput. Chem.* **1991**, *12*, 1110; b) F. Mohamadi, N. G. J. Richards, W. C. Guida, R. Liskamp, M. Lipton, C. Caufield, G. Chang, T. Hendrickson, W. C. Still, *ibid.* **1990**, *11*, 440–467; c) W. C. Still, A. Tempczyk, R. C. Hawley, T. Hendrickson, *J. Am. Chem. Soc.* **1990**, *112*, 6127–6129; d) D. Q. McDonald, W. C. Still, *ibid.* **1994**, *116*, 11550–11553.
[16] M. Kurz, D. F. Mierke, H. Kessler, *Angew. Chem.* **1992**, *104*, 213–214; *Angew. Chem. Int. Ed. Engl.* **1992**, *31*, 210–212.
[17] Crystallographic data (excluding structure factors) for the structures reported in this paper have been deposited with the Cambridge Crystallographic Data Centre as supplementary publication No. CCDC-1220-6. Copies of the data can be obtained free of charge on application to the Director, CCDC, 12 Union Road, Cambridge CB2 1EZ, UK (Fax: Int. code +(1223)336-033; e-mail: teched@chemcrys.cam.ac.uk).
[18] a) B. A. Frenz and Associates, SDP Structure Determination Package, College Station, Texas, USA, and Enraf–Nonius, Delft, The Netherlands, **1985**; b) MolEN, An Interactive Structure Solution Procedure, Enraf–Nonius, Delft, The Netherlands, **1990**.
[19] W. H. Baur, E. Tillmans, *Acta Cryst.* **1986**, *B24*, 95–111.
[20] G. Dewolff, *International Tables for X-Ray Crystallography*, *vol. A*, Reidel, Dordrecht, **1983**, pp. 737–744.
[21] A. C. T. North, D. C. Phillips, F. S. Mathews, *Acta Cryst.* **1968**, *A24*, 351–355.
[22] P. Main, S. J. Fiske, S. E. Hull, L. Lessinger, G. Germain, J.-P. Declerq, M. M. Woolfson, MULTAN80. A System of Computer Programs for the Automatic Solution of Crystal Structures from X-ray Diffraction Data, Universities of York, England, and Louvain, Belgium, **1980**.
[23] *International Tables for X-ray Crystallography*, Kynoch, Birmingham, England, **1974**, Vol. 4, pp. 99–101 and 149–150.